IN THE UNITED STATES PATENT AND TRADEMARK OFFICE
Before the Board of Patent Appeals and Interferences

AF/2643
IFW

In re Patent Application of
LINDQVIST et al.
Serial No. 09/584,796
Filed: June 1, 2000
Title: A FREQUENCY DOMAIN ECHO CANCELLER

Atty Dkt. 1410-679
C# M#
TC/A.U.: 2643
Examiner: Jamal, Alexander
Date: August 16, 2006

Mail Stop Appeal Brief - Patents
Commissioner for Patents
P.O. Box 1450
Alexandria, VA 22313-1450

Sir:

☐ **Correspondence Address Indication Form Attached.**

☐ **NOTICE OF APPEAL**
Applicant hereby **appeals** to the Board of Patent Appeals and Interferences from the last decision of the Examiner twice/finally rejecting applicant's claim(s). $500.00 (1401)/$250.00 (2401) $

☒ An appeal **BRIEF** is attached in the pending appeal of the above-identified application **Re-submitted Appeal Brief, fee previously paid July 13, 2006.** $500.00 (1402)/$250.00 (2402) $ Fee paid 7/13/06

☐ Credit for fees paid in prior appeal without decision on merits -$ ( )

☒ A Response to Notice of Non-Compliant Appeal Brief is attached. **(no fee)**

☐ Petition is hereby made to extend the current due date so as to cover the filing date of this paper and attachment(s)
One Month Extension $120.00 (1251)/$60.00 (2251)
Two Month Extensions $450.00 (1252)/$225.00 (2252)
Three Month Extensions $1020.00 (1253/$510.00 (2253)
Four Month Extensions $1590.00 (1254/$795.00 (2254) $

☐ "Small entity" statement attached.

Less month extension previously paid on -$( )

TOTAL FEE ENCLOSED $ 0.00

Any future submission requiring an extension of time is hereby stated to include a petition for such time extension. The Commissioner is hereby authorized to charge any deficiency, or credit any overpayment, in the fee(s) filed, or asserted to be filed, or which should have been filed herewith (or with any paper hereafter filed in this application by this firm) to our **Account No. 14-1140.** A duplicate copy of this sheet is attached.

901 North Glebe Road, 11th Floor
Arlington, Virginia 22203-1808
Telephone: (703) 816-4000
Facsimile: (703) 816-4100
JRL:maa

NIXON & VANDERHYE P.C.
By Atty: John R. Lastova, Reg. No. 33,149

Signature: _____

IN THE UNITED STATES PATENT AND TRADEMARK OFFICE

In re Patent Application of
LINDQVIST et al.
Serial No. 09/584,796
Filed: June 1, 2000

Atty. Ref.: 1410-679
TC/A.U.: 2643
Examiner: Jamal, Alexander

For: A FREQUENCY DOMAIN ECHO CANCELLER

* * * * * * * * * * * *

August 16, 2006

Mail Stop Non-Fee Amendment
Commissioner for Patents
P.O. Box 1450
Alexandria, VA 22313-1450

Sir:

RESPONSE TO NOTICE OF NON-COMPLIANT APPEAL BRIEF

In response to the Notice of Non-Compliant Appeal Brief (mailed August 11, 2006) and a telephone conversation with Ms. Bridget C. Monroe, Appellants re-submit the appeal brief. As requested, the status of cancelled claims 2, 8 and 29 has been included. The statement of the obviousness rejections now explicitly recites the statutory basis corresponding to 35 USC §103. Because the statute was explicitly recited in the statement of each ground of rejection presented for review, Ms. Monroe indicated that the headings under the Argument section in the originally-filed brief were acceptable. The Summary of the Claimed Invention section as originally filed contained numerous references to the specific figures, specific reference numerals in figures, as well as pages and lines in the specification text. The Summary has been further amended to include additional line number references and to specifically map the specific independent claims

to specific portions of the Summary text. As such, the newly submitted Appeal Brief is believed to overcome the issues identified in the Notification of Non-Compliant Appeal Brief. Appellants request that the appeal proceed on the merits.

Respectfully submitted,

NIXON & VANDERHYE P.C.

By: _____
John R. Lastova
Reg. No. 33,149

JRL:maa
901 North Glebe Road, 11th Floor
Arlington, VA 22203-1808
Telephone: (703) 816-4000
Facsimile: (703) 816-4100

IN THE UNITED STATES PATENT AND TRADEMARK OFFICE

In re Patent Application of

LINDQVIST et al.

Serial No. 09/584,796

Filed: June 1, 2000

For: A FREQUENCY DOMAIN ECHO CANCELLER

Atty. Ref.: 1410-679

Group: 2643

Examiner: Jamal, Alexander

Before the Board of Patent Appeals and Interferences

BRIEF FOR APPELLANT
On Appeal From Final Rejection
From Group Art Unit 2643

John R. Lastova
NIXON & VANDERHYE P.C.
11th Floor, 901 North Glebe Road
Arlington, Virginia 22203-1808
(703) 816-4025
Attorney for Appellants
Lindqvist, Fertner, Frenger (Inventors)
Telefonaktiebolaget L M Ericsson (publ)
(Assignee)

TABLE OF CONTENTS

IN THE UNITED STATES PATENT AND TRADEMARK OFFICE
BEFORE THE BOARD OF PATENT APPEALS AND INTERFERENCES

In re Patent Application of
LINDQVIST et al.
Serial No. 09/584,796
Filed: June 1, 2000
For: A FREQUENCY DOMAIN ECHO CANCELLER

Atty. Ref.: 1410-679
Group: 2643
Examiner: Jamal, Alexander

* *

August 15, 2006

Mail Stop Appeal Brief - Patents
Commissioner for Patents
P.O. Box 1450
Alexandria, VA 22313-1450

APPEAL BRIEF

I. REAL PARTY IN INTEREST

The real party in interest is the assignee, Telefonaktiebolaget L M Ericsson (publ), a Swedish corporation.

II. RELATED APPEALS AND INTERFERENCES

A pre-appeal was filed on November 9, 2005, which in accordance with a communication from the office on June 15, 2006, did not result in withdrawal of the final action. There are no other appeals related to this subject application. There are no interferences related to this subject application.

III. STATUS OF CLAIMS

Claims 1, 3-7, 9-28, and 30-44 are pending. Claims 1, 3-7, 9-17, and 20-43 stand rejected under 35 U.S.C. §103 as being unpatentable over U.S. Patent 5,317,596 to Ho in view of U.S. Patent 6,597,745 to Dowling. Claims 18, 19, and 44 stand rejected under 35 U.S.C. §103 as being unpatentable over U.S. Patent 5,117,418 to Chaffee in view of Dowling. Claims 2, 8, and 29 are cancelled.

IV. STATUS OF AMENDMENTS

No amendment has been filed after the final action.

V. SUMMARY OF THE CLAIMED SUBJECT MATTER

The independent claims 1, 12, 18, 19, 20, and 30 in this case are directed to a frequency domain echo canceller, and independent claim 35 recites a method for reducing echo at a transceiver. Beneficial example applications of the frequency domain echo cancellers and method include multicarrier modulation methods, such as DMT (Discrete MultiTone), where digital subscriber lines are employed for high speed data transmission and OFDM (Orthogonal Frequency Division Multiplexing) based systems. Figure 1 shows a "near-end" DSL modem having a transmitter 12 and a receiver 14 connected to the subscriber line's twisted-pair 18 (telephone line) via a so-called hybrid circuit 16. The transmitted signal is transmitted over a communications channel on the subscriber line to a "far-end"

DSL modem (not shown), which has its own transmitter and receiver. Because the hybrid 16 cannot be exactly matched to the impedance of the subscriber line, the transmitted signal "leaks" back into the receiver through the hybrid creating an echo signal. An echo canceller in the "near end" station may be used to cancel the echo signal. The echo canceller first estimates the echo signal from the transmitted signal, and then subtracts the estimated echo signal from the received signal. In order to estimate the echo signal, the echo canceller must model the echo path channel. (See page 1, line 9-page 2, line 7).

A DMT signal that is filtered through a physical channel is subjected to inter-symbol-interference (ISI) because all practical physical channels have "memory," i.e., a non-zero impulse response. This impairment of the physical channel causes the transmitted DMT symbols to interfere with each other (ISI). Furthermore, the transitions between the DMT symbol cause transients in the received signal. These transients cause interference between the carriers in the same DMT symbol. This type of interference is known as inter-channel interference (ICI), where the "channel" refers to the DMT subchannel. ISI and ICI are two distinct phenomena that both cause data distortion. The echo signal received at the near-end station, like the data signal transmitted over the channel and received at the far-end station, is affected by ISI and ICI, because all practical physical echo path channels have a long impulse response (memory). Thus, the

echo from one carrier will leak into every other carrier within the same DMT symbol and the next transmitted DMT symbol. (See page 3, lines 8-21).

The frequency domain echo canceller recited in independent claim 20 takes into account interchannel interference when estimating an echo signal to be removed from a received signal. The frequency domain echo canceller recited in independent claim 30 takes into account intersymbol interference and interchannel interference when estimating an echo signal to be removed from a received signal. For example, see block 50 in Figure 3. Calculating the received echo signal completely in the frequency domain is particularly beneficial in a DMT type system because the transmitted data is already available in the frequency domain. Accordingly, the echo estimate is determined using a frequency domain model of an echo path channel that includes the effects of interference like ISI and ICI. (See page 4 and page 8, lines 22-page 9, line 2).

Seven non-limiting example embodiments of a frequency domain echo canceller are disclosed and claimed. In a first example embodiment to which independent claims 1 and 18 are directed, the frequency domain model of the echo path channel is determined using a first matrix of coefficients $\mathbf{H}_i$ and a second matrix of coefficients $\mathbf{W}_i$. The first matrix is combined with a current transmitted symbol $\mathbf{X}_i$, and the second matrix is combined with a previously transmitted symbol $\mathbf{X}_{i-1}$. The sum of these two combinations is used to estimate the echo

signal $\hat{\mathbf{Y}}_i$. The coefficients of the first matrix represent how an echo from a currently transmitted frequency domain signal affects a received signal. The coefficients of the second matrix represent how an echo from a previously transmitted domain symbol affects the received symbol. The coefficients of the first and second matrices are adjusted using a difference between the received signal and the estimated signal. (See page 9, line 3-page 14, line 20 and Figures 4 and 5).

In a second example embodiment, the current transmitted symbol and the previously transmitted symbol are partitioned into real and imaginary parts before being combined with matrices as described in the first example embodiment. This operation reduces the computational complexity by a factor of two compared to the first example embodiment. (See page 14, line 21-page 17, line 9).

In a third example embodiment to which independent claims 12 and 19 are directed, the currently transmitted symbol is combined with a first column vector $\mathbf{V_i}$. The previously transmitted symbol is multiplied with a complex exponential term, $e^{j2\pi Lk/N}$, in order to compensate for the cyclic prefix, and then subtracted from the current transmitted symbol. The resulting signal is combined with a matrix $\mathbf{Z_i}$. The vector and matrix combinations are summed and used to estimate the echo signal to be removed from the received symbol. See equations 40 and 41. This third example embodiment reduces the computational complexity

approximately by a factor of two compared to the first example embodiment. (See page 17, line 10-page 18, line 17 and Figure 6). Independent method claim 35 is directed to both the first and third embodiments.

In a fourth example embodiment, the operations described in the second and third example embodiments are combined resulting in a reduction of computational complexity approximately by a factor of four compared to the first example embodiment. (See page 18, line 18-page 19, line 6).

In a fifth example embodiment, when the transmitter of a transceiver has a lower sampling rate than its receiver, the received echo signal is interpolated at the receiver. The interpolation may also be combined with the operations described in the second example embodiment to reduce the computational complexity by a factor of four compared to the first example embodiment. (See page 19, line7-page 20, line 10).

In a sixth example embodiment, when the transmitter has a higher rate than the receiver, the echo signal is decimated at the receiver. The decimation may also be combined with the operations described in the second example embodiment to reduce the computational complexity by a factor of four compared to the first example embodiment. (See page 20, line 11-page 21 line 12).

In a seventh example embodiment, when the transmitted symbols are not aligned in time with the received symbols or frames, an asynchronous echo

canceller may be used. The asynchronous echo canceller may be combined with previously-described example embodiments. (See page 22, lines 3-21).

In a DMT type modem, because all of the data is already available in the frequency domain, there is no need to do any additional Fourier transform or inverse Fourier transform operations, except for the asynchronous echo canceller embodiment which requires one extra IDFT. Moreover, some of the coefficients in the matrices may be very small and ignored, further reducing the computational complexity and memory required.

VI. GROUNDS OF REJECTION TO BE REVIEWED ON APPEAL

The two grounds of rejection to be reviewed on appeal are the obviousness rejections under 35 U.S.C. §103 based on (1) the combination of Ho in view of Dowling, and (2) the combination of Chaffee in view of Dowling.

VII. ARGUMENT

A. Ho and Chaffee Lack Multiple Claim Features

Independent claims 1, 12, 18, 19, and 35 all recite estimating echo in the frequency domain using a specific approach. The Examiner admits that Ho and Chaffee do not teach estimating the echo signals in the frequency domain using a combination of (i) a product of a first matrix (specifically a vector in claim 12) of coefficients in the frequency domain and a transmitted symbol and (ii) a product

of a second matrix of coefficients in the frequency domain and a previously-transmitted symbol.

More fundamentally, independent claims 1, 12, 18, and 19 recite "estimat[ing] in the frequency domain an echo signal" and " remov[ing] in the frequency domain the estimated echo signal in the frequency domain from a received signal in the frequency domain." Chaffee disclose an echo canceller in which the estimated echo is converted to the time-domain and subtracted from the received signal. Chaffee does not cancel echoes in the frequency domain.

Ho relies primarily on echo cancellation in the time domain. See lines 10-13 of col. 6: "After the adder **52** *subtracts the time-domain portion of the echo*, e(n), the output is converted by a serial-to-parallel (S/P) converter **54** into a block of N real-valued time-domain samples." Then a residual echo is converted from the time to the frequency domain so that a residual echo E(f) is removed. Hence, *the main echo is removed in the time-domain*, and then the result is corrected in frequency-domain. The reason Ho takes this approach is that Ho does not (and can not) remove the echo due to a previous symbol in the frequency domain.

The Examiner relies on Dowling to remedy the deficiencies in Ho and Chaffee. That reliance is misplaced.

B. Dowling Is A Pre-Equalizer—Not An Echo Canceller

Dowling describes a "pre-coder" which is a pre-equalizer—not an echo canceller. Dowling *precodes* a signal *before* the signal is transmitted in order to compensate for transmission channel distortion (not echo) that would otherwise distort the signal received at the intended receiver, i.e., the far-end station. The hope is that this precoded signal will be received without the far-end station having to equalize the signal. In other words, Dowling tries to compensate for the channel distortion before transmission over the channel so that the transmitted signal is received at the other end of the transmission channel more or less undistorted (at least in theory). So Dowling is concerned about the signal received at the far-end station. Compensating for the distortion caused by a transmission channel is an entirely different problem as compared to canceling an echo.

In contrast, the claimed echo cancellation is at the near-end station, and the echo that the near-end station must deal with is reflected back through an echo path to the near-end station. These basic facts would be well understood by those skilled in echo cancellation.[1] While Dowling effectively pre-equalizes (precodes) the transmitted signal for the transmission channel in order to simplify signal processing in the far-end station, the instant claims remove echo in the near-end

[1] For a brief background regarding echo cancellation, please see pages 1 and 2 of the instant specification and Figure 1.

station caused by the near-end transmitted signal. These are two very different operations responding to two different problems.

C. Compensating For Channel Distortion Does Not Compensate For Echo

Dowling's precoder does not estimate and remove an echo signal from a received signal—let alone do this in the frequency domain. Rather, Dowling estimates and "removes" the expected transmission channel distortion from the transmitted signal so that distortion introduced by the transmission channel will be minimized at the far-end station receiver. Dowling's channel distortion estimate ***does not include echo cancellation***. Echo is caused by transmission line impedance mismatches, which is different from the channel transfer function. Echo is experienced at the near-end station transmitter, and not at the far-end station receiver, which is the intended beneficiary of Dowling's precoding. Why would Dowling model/estimate an echo that is not part of the channel distortion of the signal received at the far-end station receiver? Echo is a problem for the near-end station to deal with and not the far-end station.

The Examiner relies on col. 22, lines 1-3, where Dowling states that "communication systems often involve other elements such as echo cancellers which may be advantageously merged with the precoder." But here *Dowling admits that his precoder/pre-equalizer does not perform echo cancellation.* If echo is to be canceled, Dowling explicitly states that an echo canceller is needed

because his precoder does not cancel echo. Thus, the Examiner's premise that Dowling's precoder some how removes the echo from the transmitted signal cannot stand.

D. The Ho/Chaffee/Dowling Combinations Fall Short.

Even if Dowling's precoder were "merged" with Ho's or Chaffee's echo canceller, one would not arrive at the claimed echo cancellation. Dowling's precoder, by Dowling's own admission, does not perform echo cancellation. Hence, in the Examiner's proposed combination, it is just Ho's echo canceller or Chaffee's echo canceller doing the echo cancellation, which the Examiner rightly admits is not the claimed echo cancellation. So the proposed combination fails.

To cancel echo, (which is not transmitted over the transmission channel), a model of the echo is needed; however, a model of the transmission channel is not. On the other hand, Dowling's precoding modifies the transmitted signal using an inversion of the *transmission channel* transfer function (not an echo channel transfer function). The hoped for result is the receiver gets a signal that is more or less unaffected by the transmission channel transfer function. But only knowledge of the transmission channel is needed and not the echo experienced at the near-end station. And in the merged combination of Ho and Dowling or Chaffe and Dowling, where Dowling's precoder is used along with a separate and distinct

echo canceller, the echo is removed from the transmitted signal in a conventional way rather than as claimed.

E. The Ho/Chaffee/Dowling Combinations Would Not Be Made By A Person Of Ordinary Skill In The Art

Notwithstanding the significant deficiencies already noted, assume for the sake of argument that there was some provision by Dowling to precode the signal to be transmitted for echo cancellation—which Dowling plainly does not do—along with precoding for the transmission channel. The echo would be modeled and then inverted (call this X) just like the transmission channel is modeled and inverted (call this Y). But the consequence is that the inverted echo model X negatively affects the inverted channel model Y resulting in distorting the received signal even more at the far-end station receiver. For this reason alone, a person skilled in this art would not make this modification.

Moreover, further distorting of the signal at the far-end receiver and the need for more sophisticated equalization at the far-end receiver are the very things Dowling is trying to avoid. Dowling's title is "Reduced Complexity Multicarrier Precoder," and column 2, lines 41-42 state: "The foregoing indicates a recognized but unmet need for a reduced complexity DMT-THP [a DMT-THP is defined in column 1, lines 23-24 as "a transmitter-based precoder structure"]." Thus, the Examiner requires in the combinations upon which the final rejections are based a

modification that renders Dowling inoperable for Dowling's consistently articulated and intended purpose. This thwarting of Dowling's primary purpose is a clear indicator of an inappropriate obviousness rejection. *In re Gordon*, 733 F.2d 900, 902 (Fed. Cir. 1984).

Consider an alternative combination where Dowling's precoded signal is directly applied to the input of Ho's echo canceller. In this case, that applied signal is still only compensated for transmission channel ISI and ICI. The echo ISI and ICI would not be compensated for, but instead would be additionally distorted. Accordingly, Ho's echo canceller cannot be combined with Dowling's precoder in the manner proposed by the Examiner to result in the claimed echo canceller. Such a proposed combination certainly does not result in estimating a echo signal in the frequency domain using the claimed combination of first and second matrices with a transmitted symbol and a previously-transmitted symbol.

These significant obstacles and inconsistencies with trying to combine Dowling with Ho and with Chaffee demonstrate that the requisite motivation to combine is missing. A proper motivation to combine requires an appreciation of the desirability of making the combination. It is not measured by the feasibility of making the combination. See *Winner Int'l Royalty Corp. v. Wang*, 202 F.3d 1340, 1349 (Fed. Cir. 2000). In this case, the combination has been shown to be both undesirable and infeasible.

Still further, the Examiner must show reasons that the skilled artisan, confronted with *the same problems* as the inventor and *no knowledge of the claimed invention*, would select the elements from the cited prior art references for the combination in the manner claimed. *In re Rouffet*, 149 F.3d 1350, 1357 (Fed. Cir. 1998). None of Ho, Chaffee, or Dowling reduces the negative affects of ICI and ISI in echo cancellation using a frequency domain echo canceller.

F. Ho And Dowling Do Not Compensate for Echo ICI or ISI

The features recited in claims 20 and 30 are not taught in the combination of Ho and Dowling. The frequency domain echo canceler in claim 30 "estimate[s] the echo in the received signal using *a frequency domain model of an echo path* channel that *includes effects of intersymbol interference and inter-carrier interference and to subtract the echo estimate from the received signal* to provide a difference." See also claims 20 and 21. Neither Ho nor Dowling teaches an echo canceller that takes into account effects of **echo** inter-carrier interference (ICI) and inter-symbol interference (ISI) in a frequency domain model of an echo estimate so that it can be subtracted out from the received echo at the near-end station.

The Examiner assumes that ICI is a form of either ISI or noise. To the contrary, as explained in the background of this application, ICI is not the same as ISI. Nor is ICI simply "noise." The two articles previously-provided to the Examiner and attached in the Evidence Appendix confirm this.

Another fundamental point ignored by the Examiner is that the ISI and ICI in the transmitted signal sent over the transmission channel are not the same as the ISI and ICI in the echo. None of the applied references model or compensate for the **echo** ISI and **echo** ICI.

Still further, the rejection of claims 20 and 30 is improper because the combination of Ho and Dowling cannot be properly made for the myriad reasons already explained.

VII. CONCLUSION

Multiple features of the independent claims are not disclosed or suggested by the combination of Ho and Dowling or Chaffee and Dowling. Nor is there proper motivation to combine their teachings as the Examiner proposes. Each missing claim feature and the lack of motivation for each combination is an independent ground for reversal. The Board should reverse the outstanding rejections.

Respectfully submitted,

NIXON & VANDERHYE P.C.

By: 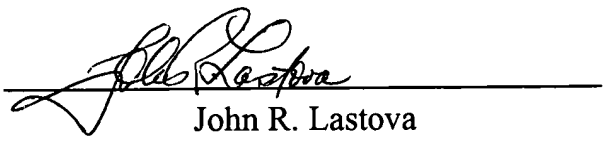

John R. Lastova
Reg. No. 33,149

JRL/maa
Enclosures

IX. CLAIMS APPENDIX

1. An echo canceller for use in a transceiver, comprising:

first electronic circuitry configured to estimate in the frequency domain an echo signal, and

second electronic circuitry configured to remove in the frequency domain the estimated echo signal in the frequency domain from a received signal in the frequency domain,

wherein the first electronic circuitry is further configured to estimate the echo signals in the frequency domain using a combination of (i) a product of a first matrix of coefficients in the frequency domain and a transmitted symbol and (ii) a product of a second matrix of coefficients in the frequency domain and a previously-transmitted symbol.

3. The echo canceller in claim 1, wherein transmitted signals corresponding to the transmitted symbol and the previously-transmitted symbol are real-valued, and wherein the transmitted symbol and the previously-transmitted symbol are divided into real and imaginary parts before being combined with the respective matrix to reduce computational complexity.

4. The echo canceller in claim 1, wherein the coefficients of the first matrix represent how an echo from a currently transmitted frequency domain signal affects a received signal.

5. The echo canceller in claim 4, wherein the coefficients of the second matrix represent how an echo from a previously transmitted frequency domain signal affects the received signal.

6. The echo canceller in claim 1, wherein the first electronic circuitry is further configured to adapt the coefficients of the first matrix and the second matrix using a difference between the received signal and the estimated echo signal.

7. The echo canceller in claim 6, wherein the first electronic circuitry is further configured to adapt the coefficients using a least mean squares algorithm.

9. The echo canceller in claim 1, wherein the transceiver is a discrete multitone (DMT) transceiver.

10. The echo canceller in claim 1, wherein the first and second matrices are N x N matrices, where N is a number of symbol samples.

11. The echo canceller in claim 1, wherein a vector corresponding to a transmitted frequency domain symbol, a vector corresponding to a received frequency domain signal, and a vector corresponding to an estimate of the echo symbol are all Hermitian symmetric.

12. The echo canceller for use in a transceiver, comprising:

first electronic circuitry configured to estimate in the frequency domain an echo signal, and

second electronic circuitry configured to remove in the frequency domain the estimated echo signal in the frequency domain from a received signal in the frequency domain,

wherein the first electronic circuitry is further configured to estimate the echo signals in the frequency domain using a combination of a product of (i) a vector of coefficients in the frequency domain and a transmitted symbol and (ii) a product of a matrix of coefficients in the frequency domain and a compensated, previously-transmitted symbol .

13. The echo canceller in claim 12, wherein the first electronic circuitry is further configured to divide the transmitted symbol and the previously-transmitted symbol into real and imaginary parts before combining them respectively with the vector and the matrix to reduce computational complexity.

14. The echo canceller in claim 12, wherein a compensation factor used to compensate the previously-transmitted signal is a complex exponential term.

15. The echo canceller in claim 14, wherein the transceiver is a discrete multitone (DMT) transceiver and the compensation factor compensates for a cyclic prefix associated with the previously-transmitted signal.

16. The echo canceller in claim 1, wherein when a transmitter of the transceiver has a lower sampling rate than a receiver of the transceiver, the echo signal is interpolated at the receiver.

17. The echo canceller in claim 1, wherein when a transmitter of the transceiver has a higher sampling rate than a receiver of the transceiver, the echo signal is decimated at the receiver.

18. An echo canceller for use in an asynchronous transceiver configured to cancel an echo signal, comprising:

a first matrix of coefficients;

a second matrix of coefficients; and

electronic circuitry configured to use a combination of (i) a product of the first matrix and a currently-transmitted symbol and (ii) a product of the second matrix and a previously-transmitted symbol to estimate an echo signal in the frequency domain, to transform the estimate of the echo signal into the time domain, and to remove the transformed estimate from a received signal in the time domain.

19. An echo canceller for use in an asynchronous transceiver configured to cancel an echo signal, comprising:

a vector of coefficients in the frequency domain;

a matrix of coefficients in the frequency domain,

electronic circuitry configured to use a combination of (i) a product of the vector and a currently-transmitted symbol and (ii) a product of the matrix and a compensated, previously-transmitted symbol to estimate an echo signal in the frequency domain, to transform the estimated echo signal into the time domain, and to remove from a received signal in the time domain.

20. An echo canceller for use in a transceiver canceling an echo from a received signal in the frequency domain including circuitry configured to determine an estimate of the echo in the received signal using a frequency domain model of an echo path channel that takes into account effects of inter-carrier interference and to subtract the echo estimate from the received signal.

21. The echo canceller in claim 20, wherein the echo canceller is used in a discrete multitone (DMT) type transceiver and the frequency domain model takes into account intersymbol interference .

22. The echo canceller in claim 20, wherein the frequency domain model includes a first set of values that models how an echo from a currently transmitted frequency domain symbol distorts the received signal and a second set of values that models how an echo from a previously transmitted frequency domain symbol distorts the received signal.

23. The echo canceller in claim 22, wherein the first set of values is a first complex matrix and the second set of values is a second complex matrix.

24. The echo canceller in claim 22, wherein the first set of values is a column vector and the second set of values is a matrix.

25. The echo canceller in claim 24, wherein the matrix is combined with a difference between the currently transmitted symbol and a product of the previously transmitted symbol and a compensating factor.

26. The echo canceller in claim 22, wherein the transmitted symbol and the previously transmitted symbol are divided into real and imaginary parts before being combined with the first and second sets of values, respectively.

27. The echo canceller in claim 20, wherein when a transmitter of the transceiver has a lower sampling rate than a receiver of the transceiver, the echo signal is interpolated at the receiver.

28. The echo canceller in claim 20, wherein when a transmitter of the transceiver has a higher sampling rate than a receiver of the transceiver, the echo signal is decimated at the receiver.

30. A frequency domain echo canceller for use in a transceiver canceling an echo from a received signal in the frequency domain including circuitry configured to determine an estimate of the echo in the received signal using a frequency domain model of an echo path channel that includes effects of intersymbol interference and inter-carrier interference and to subtract the echo estimate from the received signal to provide a difference.

31. The echo canceller in claim 30, wherein the frequency domain model includes a first set of values that models completely in the frequency domain how an echo from a currently transmitted frequency domain symbol distorts the received signal and a second set of values that models completely in the frequency domain how an echo from a previously transmitted frequency domain symbol distorts the received signal.

32. The echo canceller in claim 31, wherein transmitted signals corresponding to the currently and previously transmitted frequency domain symbols are real-valued.

33. The echo canceller in claim 32, wherein the currently transmitted symbol, the previously transmitted symbol, the received signal, and the difference are vectors having Hermitian symmetry.

34. The echo canceller in claim 31, wherein the difference is used to adjust the first and second set of values.

35. A method for reducing an echo at a transceiver comprising:

(a) combining in the frequency domain a currently-transmitted symbol with a first vector or matrix of coefficients in the frequency domain resulting in a first combination;

(b) combining in the frequency domain a previously-transmitted symbol with a second matrix of coefficients in the frequency domain resulting in a second combination;

(c) combining the first and second combinations in the frequency domain to estimate the echo in the frequency domain; and

(d) using the estimated echo to reduce the echo in a signal received at the transceiver.

36. The method in claim 35, further comprising:

determining a difference between the received signal and the estimated echo, and

adjusting the first and second set of values using the difference.

37. The method in claim 35, wherein the first vector or matrix corresponds to a first matrix of coefficients .

38. The method in claim 35, wherein the first vector or matrix corresponds to a column vector of coefficients .

39. The method in claim 38, wherein the combining step (b) includes:

multiplying the previously transmitted symbol by a compensation factor to produce a product;

subtracting the product from the currently transmitted symbol; and

combining a result of the subtracting with the matrix.

40. The method in claim 35, wherein when a transmitter of the transceiver has a lower sampling rate than a receiver of the transceiver, the method further comprising:

interpolating the echo signal.

41. The method in claim 35, wherein when a transmitter of the transceiver has a higher sampling rate than a receiver of the transceiver, the method further comprising:

decimating the echo signal.

42. The method in claim 35, wherein a vector corresponding to a transmitted frequency domain symbol, a vector corresponding to a received frequency domain signal, a vector corresponding to an estimate of the echo symbol are Hermitian symmetric.

43. The method in claim 35, further comprising:

dividing the currently transmitted symbol and the previously-transmitted symbol into real and imaginary parts before the combining steps (a) and (b), respectively, to reduce computational complexity.

44. The method according to claim 35, wherein the transceiver is an asynchronous transceiver, the method further comprising:

transforming the estimated echo into the time domain, and

removing in the time domain, the estimated echo signal from the received signal on a sample-by-sample basis.

X. EVIDENCE APPENDIX

Two articles are attached that were submitted to the Examiner on June 15, 2005 and are referred to in the argument section above: "A Novel Intercarrier Interference Cancellation Approach in OFDM based on BSS," by Liu et al and "Residual Frequency Offset Correction for Coherently Modulated OFDM Systems in Wireless Communication," by Abhayawardhana et al.

XI. RELATED PROCEEDINGS APPENDIX

There is no related proceedings appendix.

Residual Frequency Offset Correction for Coherently Modulated OFDM Systems in Wireless Communication

V.S. Abhayawardhana, I.J. Wassell
Laboratory for Communications Engineering,
Department of Engineering, University of Cambridge, UK
{vsa23,ijw24}@eng.cam.ac.uk

Abstract—**Orthogonal Frequency Division Multiplex (OFDM) systems are very sensitive to frequency offset caused by tuning oscillator instabilities and Doppler shifts induced by the channel. The Schmidl and Cox Algorithm (SCA) is quite robust in estimating the frequency offset for systems with large OFDM symbol lengths. It uses two OFDM symbols for training with the first one having two identical halves. The frequency offset is estimated by correlating a received sequence of samples equal to half the OFDM symbol length with the following received samples. The effect of Additive White Gaussian Noise (AWGN) in the estimation process is mitigated only if the number of samples used in the correlation, and hence the OFDM symbol size is large. However to be successfully applied to Broadband Fixed Wireless Access (BFWA) systems, OFDM should perform well even with smaller symbol lengths. In this paper we present the Residual Frequency Offset Correction Algorithm (RFOCA), which uses the SCA for initial frequency offset acquisition and follows it with a stage which reduces the initial residual frequency offset by tracking the phase of the decoded data. We show through simulation that the RFOCA achieves an error variance that is many orders of magnitude lower than at the end of the acquisition stage using the SCA alone.**

I. Introduction

Various solutions have been suggested as contenders to overcome the challenge of transmitting data to the subscriber at high data rates demanded by future broadband applications, for example Broadband Fixed Wireless Access (BFWA), Digital Subscriber Lines (DSL), Cable Modems and Satellite Communication. This paper will address BFWA, owing to its advantages of ease of deployment and cost. Orthogonal Frequency Division Multiplex (OFDM) has been the most popular physical layer standard for BFWA systems due to its robustness and efficiency mainly because it uses a simple Fast Fourier Transform (FFT) of finite length N for modulation and demodulation. Among the standards that have placed their confidence in OFDM are HIPERLAN-2 [1] and IEEE 802.11-a [2].

The orthogonality of the consecutive OFDM symbols is maintained by appending a length v cyclic prefix (CP) at the start of each symbol [3]. The CP is obtained by taking the last v samples of each symbol and consequently the total length of the transmitted OFDM symbols is $(N+v)$ samples. For each OFDM symbol to be independent and to avoid any Inter Symbol Interference (ISI) or Inter Carrier Interference (ICI), the length of the Channel Impulse response (CIR) should be less than $v+1$ samples. Hence the distortion caused by the CIR only affects the samples within the CP. The receiver discards the CP and takes only the last N samples of each OFDM symbol for demodulation by the receiver FFT. In such a case, the linear convolution of the transmitted signal with the CIR is converted into a circular one. Consequently, for coherently modulated OFDM systems the effects of the CIR can then be equalized by an array of one-tap Frequency Domain Equalizers (FEQ) following the FFT. This is because the frequency selective fading channel can be approximated by a sum of flat fading channels, provided the number of subchannels is large enough. Sometimes a Time Domain Equalizer (TEQ) may be used to shorten the effect of the CIR [4]. Figure 1 shows the block diagram of the system, where P/S and S/P represent the Parallel to Serial and Serial to Parallel functions respectively.

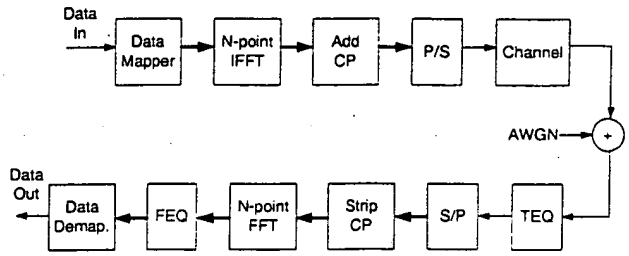

Fig. 1. Block Diagram of the OFDM System

Unfortunately, OFDM has been proven to be very sensitive to frequency offset and phase noise caused by tuning oscillator inaccuracies or Doppler shifts induced by the channel. The usual deployment scenario for a BFWA system employs a point to multipoint configuration. Here, a single base station (BS) transmits data in short bursts to many subscriber units (SUs) placed at the user locations. The economic feasibility of a BFWA deployment depends heavily on the cost of the SUs. The use of low cost components, particularly the oscillators, is a major issue since their accuracy and stability are directly related to cost. Hence it is imperative that if OFDM is to be used for BFWA transmission, it should be able to operate effectively using oscillators with only moderate performance and cost.

An OFDM system effectively consists of N sinusoidal subcarriers with frequency spacing $1/T$, where T is the active symbol period of each subcarrier. The kth subcarrier will thus be at $f_k = f_0 + k/T$, where f_0 is a reference frequency. Without loss of generality, we can assume $f_0 = 0$. The modulated subcarriers overlap spectrally, but since they are orthogonal over a symbol duration, they can be easily recovered as long as the channel does not destroy the orthogonality. An unwindowed OFDM system has rectangular symbol shapes. Hence, in the frequency domain the individual subchannels will have the form of sinc functions where the first sidelobe is only some 13 dB below the main lobe of the subcarrier. In the event of a frequency offset between the transmitter and the receiver the subchannels will not align. The effect of frequency offset is two fold, it will reduce the signal power of the desired subchannel outputs and also introduce ICI further increasing the interference levels. The ICI power can be significant even for small frequency offsets in OFDM due to the high sidelobe power of the subchannels. Thus the reduction of frequency offset is critical in OFDM systems. This paper is organised as follows,

section II analyses the effect of frequency offset in OFDM analytically. Section III briefly introduces the Schmidl and Cox Algorithm (SCA) [5] and section IV introduces the novel Residual Frequency Offset Correction Algorithm (RFOCA) that compliments the SCA and improves the performance. Section V shows results obtained by computer simulation and section VI concludes and proposes future work.

II. Effect of Frequency Offset in OFDM

All analysis and simulations in this paper are performed in the digital complex baseband domain. The nth sample of the mth OFDM symbol generated by the Inverse FFT (IFFT) at the transmitter is

$$s_{m,n} = \sqrt{\frac{1}{N}} \sum_{k=0}^{N-1} A_{m,k} e^{j2\pi \frac{kn}{N}},\ 0 \le n \le N-1 \qquad (1)$$

$A_{m,k}$ is the data symbol modulated on to the kth subcarrier of the mth OFDM symbol. The data is converted into a serial sequence, then the CP of length v is added. Thus the mth transmitted OFDM symbol is $\underline{s}(m) = [s_{m,N-v}, .., s_{m,N-1}, s_{m,0}, .., s_{m,N-1}]^T$. The receiver discards the samples of the CP and uses the samples of the active OFDM symbol for decoding. We assume a finite length CIR with N_h samples, $\underline{h} = [h_0, .., h_{N_h-1}]^T$, where $v \ge N_h - 1$. We assume that N is large enough such that the frequency selective channel is divided into contiguous flat fading subchannels. If we assume that correct frame and timing synchronisation is achieved, then the received sequence after stripping the CP can be expressed as,

$$r_{m,n} = \sqrt{\frac{1}{N}} \left\{ \sum_{k=0}^{N-1} A_{m,k} H_k e^{j2\pi \frac{n(k+\epsilon)}{N}} \right\} + w_n \qquad (2)$$

for $0 \le n \le N-1$. Here H_k is the transfer function of the channel at the subchannel index k, w_n is the Additive White Gaussian Noise (AWGN) term and ϵ is the frequency offset relative to the intercarrier spacing. The symbol after FFT demodulation is

$$Y_{m,l} = \sqrt{\frac{1}{N}} \sum_{n=0}^{N-1} r_{m,n} e^{-j2\pi \frac{ln}{N}},\ 0 \le l \le N-1 \qquad (3)$$

Substituting (2) into (3) allows the output of the lth subchannel to be expressed as the sum of three components.

$$Y_{m,l} = (A_{m,l} H_l) \frac{\sin(\pi\epsilon)}{N \sin(\pi\epsilon/N)} e^{j\pi\epsilon \frac{N-1}{N}} + I_l + W_l \qquad (4)$$

The first term on rhs of equation 4, denoted R_l hereafter, shows that the desired term $A_{m,l} H_l$ experiences amplitude reduction and phase distortion. As $N \gg \pi\epsilon$, $N \sin(\pi\epsilon/N)$ can be approximated by $\pi\epsilon$. Hence the degradation of the required term vanishes when the received data does not experience any frequency offset. In practice, the effect of the channel transfer function H_l is removed by the FEQ following the FFT. Note that the FEQ is trained by transmitting a known training symbol occupying the OFDM symbol number N_t, $\underline{A} = [A_{N_t,0}, .., A_{N_t,N-1}]^T$. Usually the training symbol is placed at the beginning of the frame. The ratio of the decoded samples of the training symbol $Y_{N_t,l}$, to the locally generated copy of $A_{N_t,l}$, where $0 \le l \le N-1$, is used to calculate the coefficients for the FEQ.

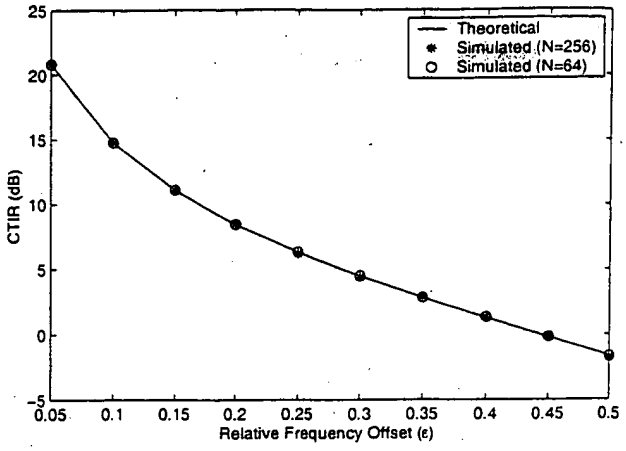

Fig. 2. Analysis of CTIR vs Relative Frequency Offset, ϵ

The second term in equation (4) is the ICI and the third term is due to the AWGN. The ICI term is given as,

$$I_l = \sum_{\substack{k=0 \\ k \ne l}}^{N-1} (A_{m,k} H_k) \frac{\sin \pi(k+\epsilon-l)}{N \sin \pi(k+\epsilon-l)/N} e^{j\pi(k+\epsilon-l)\frac{N-1}{N}} \qquad (5)$$

If we assume that the transmitted data is zero mean and uncorrelated (i.e. $E[A_{m,k}] = 0$ and $E[A_{m,l} A^*_{m,k}] = |A|^2 \delta_{l,k}$), then $E[I_l] = 0$. Hence the ICI power is,

$$E[|I_l|^2] = |A|^2 [\sin \pi\epsilon]^2 \sum_{\substack{k=0 \\ k \ne l}}^{N-1} \frac{E[|H_k|^2]}{[N \sin \pi(k+\epsilon-l)/N]^2} \qquad (6)$$

To appreciate the severity of frequency offset on the Carrier to Interference Ratio (CTIR) in an OFDM system, we define CTIR $= E[|R_l|^2]/E[|I_l|^2]$. Assuming the channel transfer function, H is unity and with zero AWGN, (i.e. $W_l = 0$), then

$$\text{CTIR} = \frac{\sum_{\substack{k=0 \\ k \ne l}}^{N-1} 1/[N \sin \pi(k+\epsilon-l)/N]^2}{[N \sin(\pi\epsilon/N)]^2} \qquad (7)$$

A similar analysis on the effect of frequency offset on OFDM can be found in [6] and [7]. Figure 2 shows CTIR in decibels as a function of ϵ. Simulated values for $N = 64$ and 256 using QPSK data mapping are also shown. It shows that the CTIR drops significantly when relative frequency offset, ϵ increases beyond 0.1. An important observation is that the CTIR is independent of N.

III. Schmidl and Cox Algorithm (SCA)

One of the more robust schemes to estimate both frame synchronisation and frequency offset is the SCA. It uses two training symbols with the first one having a repetition within half a symbol period. Frame synchronisation is achieved by searching for a training symbol with two identical halves. If $L = N/2$, the sum

of L consecutive correlations between pairs of samples spaced L apart is found as,

$$P(d) = \sum_{n=0}^{L-1} (r^*_{d+n} r_{d+n+L}) \tag{8}$$

The output of the correlator, as given by (8) will reach a peak at the end of the CP of the first training symbol. If $v > N_h - 1$ and $p = v - (N_h - 1)$, the peak is actually maintained for p samples just before the end of the CP of the first training symbol. Thus the correlator output will take the form of a plateau. This is because the last few samples of the CP, equal to the length of p, are not corrupted by the CIR. Timing synchronisation is achieved by locating the end of this plateau, denoted by d_{opt}. Since the CP ensures that there is no Inter Block Interference (IBI) between OFDM symbols, the effect of the CIR in the first training symbol is cancelled if the conjugate of a sample from the first half is multiplied by the corresponding sample from the second half. Hence the phase difference between the two halves of the first training symbol is caused by the frequency offset, $\phi = \pi\epsilon$. It can be estimated as $\hat{\phi} = 1/p \sum_{n=0}^{p} \angle P(d_{opt} - n)$. If $\epsilon < 1$ there is no phase ambiguity in $\hat{\phi}$ and the frequency offset can be estimated as

$$\hat{\epsilon}_{SCA} = \hat{\phi}/\pi \tag{9}$$

In order to resolve potential ambiguity use can be made of the second training symbol, as detailed in [5]. The effect of AWGN on the partial estimation given by equation (9) is insignificant only if L, and hence the number of FFT points N, is large. The SCA performs well for OFDM systems with N in excess of 1000 [5]. For BFWA systems, data is transmitted in short bursts, particularly in the uplink. In this situation, it would be wasteful to use an OFDM system with large N. Besides large values of N will give rise to the additional problems of high peak-to-average power ratio and will also introduce latency which reduces protocol efficiency. Typically BFWA systems utilise lower values of N such as 64 to 256 as presented in [1] and [2]. When the SCA is used for systems with lower values of N, the estimate $\hat{\epsilon}$ is not sufficiently accurate. This error results in a residual frequency offset that rotates the received constellation at a reduced rate, but one that is still significant enough to cause bit errors in coherently demodulated OFDM systems. In this paper we present the Residual Frequency Offset Correction Algorithm (RFOCA) that compliments the SCA by following it with a tracking function that continuously compensates for the residual frequency offset error.

Other approaches that are used for frequency offset correction include for example the use of null symbols [8]. The use of a null symbol is not practical in a burst mode system as the transmission will always be a null while no data is transmitted. Other suggestions utilise the correlation between the cyclic prefix and the last few samples of the OFDM symbol [9] and the self-cancellation schemes presented in [10] and [7], where the same data is sent in more than one subchannel. Both schemes are not very practical when N is a low value with the latter two approaches having the additional problem of reducing the number of useful subchannels by at least half. Note that the RFOCA does not utilise any pilots nor null symbols yet will be shown to effectively eliminate the residual offset. The proposal in [11] also attempts to track the

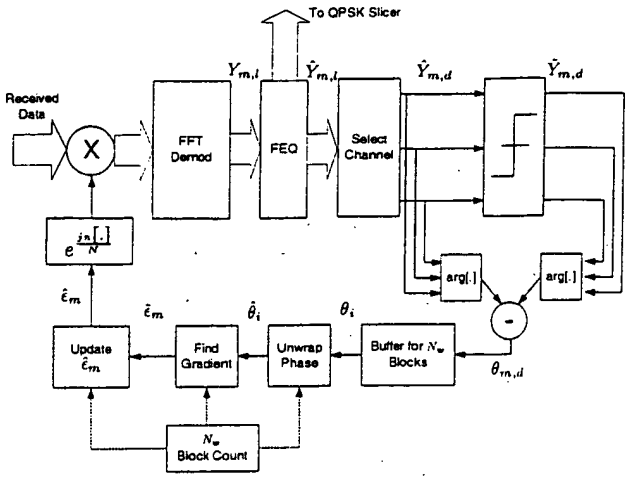

Fig. 3. Residual Frequency Offset Correction Algorithm (RFOCA)

residual frequency offset. Here, the residual offset correction factor is updated at the end of each OFDM symbol. However our tests indicate that the estimate is not very accurate when only one symbol is used, hence we update the residual offset correction factor only after analysing a block of N_w, ($N_w > 1$) OFDM symbols.

IV. Residual Frequency Offset Correction Algorithm (RFOCA)

In the proposed approach, an initial frequency offset acquisition is made using the SCA. We propose to estimate the residual frequency offset, $\bar{\epsilon}$ by tracking the rate of phase change at the FEQ outputs, $\hat{Y}_{m,l}$ as shown in Figure 3. However, the estimate of $\bar{\epsilon}$ could be seriously affected by subchannels with a low SNR resulting from spectral nulls in the channel response H_l. An estimate of H_l is made by taking the ratio of the transmitted and decoded output of the second training symbol of the SCA. Hence we only select those subchannels with $|H_l|$ above a certain threshold. We call this subset of subchannels $\underline{d} \subset [0, ..N-1]$. The criteria applied is to select subchannels with $|H_l|$ in excess of a standard deviation above the mean. For symbol m, the outputs of these subchannels $\hat{Y}_{m,d}$ are sent through a slicer to obtain $\tilde{Y}_{m,d}$, where $d \in \underline{d}$.

For symbol m the phase errors between $\hat{Y}_{m,d}$ and $\tilde{Y}_{m,d}$, namely $\theta_{m,d}$ are found as,

$$\theta_{m,d} = \angle \hat{Y}_{m,d} - \angle \tilde{Y}_{m,d} \tag{10}$$

The phase errors are stored in a buffer, $\underline{b}$ for a block of N_w OFDM symbols. Note that only the selected subchannels will be stored. Hence if the number of subchannels selected in $\underline{d}$ is N_d then the length required for the buffer is only $N_d N_w$. The Maximum Likelihood (ML) estimate of the residual frequency offset $\bar{\epsilon}$ is calculated as the gradient of the values stored in the buffer. Note, in this paper we have assumed QPSK data mapping though the technique could be extended to other constellations. Initially, $\bar{\epsilon}$ can be quite high and if the values of the phase errors, $\theta_{m,d} > \pi/4$, then it results in decoding errors being produced by the slicer which subsequently results in phase wrapping of $\theta_{m,d}$ at $\pm\pi/4$. Hence it is imperative that we first unwrap $\theta_{m,d}$ before the calculation of

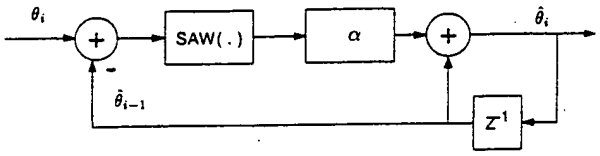

Fig.4. Phase Unwrapping Algorithm

$\tilde{\epsilon}$. Although accurate phase unwrapping algorithms are available, they are very complex. Since we are only interested in the phase gradient and not the exact phase values, a simpler scheme was selected for the unwrapping of the phase [12]. For purposes of clarity, we denote the ith sample of the wrapped phase and the unwrapped phase as θ_i and $\hat{\theta}_i$, respectively. The phase unwrapping algorithm can be expressed as

$$\hat{\theta}_i = \hat{\theta}_{i-1} + \alpha \text{SAW}(\theta_i - \hat{\theta}_{i-1}) \tag{11}$$

where SAW(.) is a sawtooth function that limits the output to $\pm\pi/4$ and α is a parameter that controls the variance of the unwrapped phase. The algorithm is illustrated in Figure 4.

The error due to frequency offset is compensated by multiplying the pre-FFT received symbols, $r_{m,n}$ with $e^{jn\hat{\epsilon}_m/N}$, where in general $\hat{\epsilon}_m$ is the frequency offset correction factor for symbol m, which is initialised to $\hat{\epsilon}_{SCA}$ at the acquisition stage. At symbol number qN_w, $\hat{\epsilon}_{qN_w}$ is updated according to $\hat{\epsilon}_{qN_w} = \hat{\epsilon}_{qN_w-1} + \tilde{\epsilon}_{qN_w}$, where q is an positive integer. For OFDM symbols $[(q-1)N_w, qN_w - 1]$, $\hat{\epsilon}_{(q-1)N_w}$ is used as the frequency offset correction factor. In other words $\hat{\epsilon}_m$ is updated once every N_w OFDM symbol blocks.

The choice of N_w is critical as a large value will cause the updating of $\hat{\epsilon}_m$ with too high a latency. However after a few updates the values of $\tilde{\epsilon}$ are quite small, hence to get a better estimate in the presence of AWGN a larger value of N_w will reduce the variance. The RFOCA can be summarised as follows.

1. Do an initial frequency offset acquisition $\hat{\epsilon}_{SCA}$ using the SCA.
2. Select the subset of subchannels with magnitudes exceeding the defined threshold in the channel transfer function, $\underline{d}$, at the start of the burst.
3. Obtain $\hat{Y}_{m,d}$ from the FEQ output and then $\tilde{Y}_{m,d}$ by use of a slicer for each symbol m, where $d \in \underline{d}$. Calculate and store $\theta_{m,d}$ for a block of N_w OFDM symbols.
4. Find the unwrapped phase $\hat{\theta}$ from the wrapped phase θ. Find the gradient of $\hat{\theta}$, namely $\tilde{\epsilon}$. This process is done once every N_w symbols.
5. Once every N_w OFDM symbol block, calculate the new frequency offset correction factor $\hat{\epsilon}_{qN_w}$.

V. Simulation Parameters and Results

OFDM systems with $N = 64, 128, 256$ have been simulated at a sampling rate of 20 MHz with a guard interval equal to 20 samples, thus the subcarrier spacings are approximately 312 kHz, 156 kHz and 78 kHz respectively. QPSK mapping for all subchannels has been employed and all the subchannels are used. A burst of 320000 data bits is assumed to be transmitted. Each data point in the simulation results is obtained by averaging over 500 such bursts. In order to test the performance of the RFOCA with frequency offset alone, we have assumed perfect symbol and frame

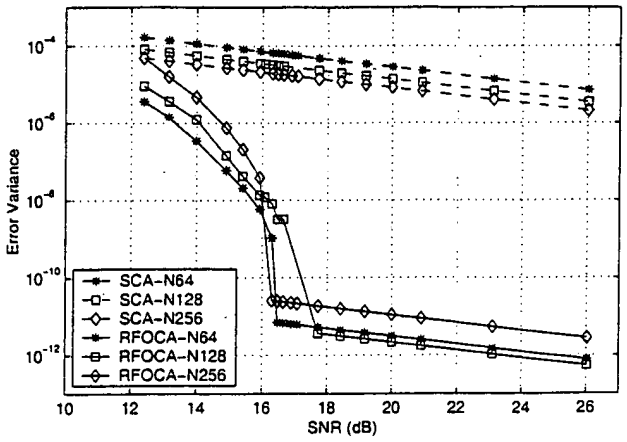

Fig. 5. Comparison of Error Variances of SCA and RFOCA in AWGN for $N = 64, 128, 256$ and $\epsilon = 0.5$

synchronisation for the simulated coherent OFDM systems. A more robust symbol synchronisation algorithm that virtually guarantees perfect frame synchronisation will be the subject of a future publication. After much testing, the values selected for N_w were $250, 250, 125$ for $N = 64, 128, 256$, respectively. Figure 5 shows the comparison of error variances at the end of the acquisition stage using the SCA and the tracking stage using the RFOCA for $N = 64, 128, 256$ as a function of the Signal to Noise Ratio (SNR), with $\epsilon = 0.5$. It shows that the RFOCA error variance is many orders of magnitude lower than at the end of the acquisition stage. There appears to be a threshold effect in RFOCA at around an SNR of 16 dB, below which the error variance increases rapidly. It is mainly due to the errors present in the selected subchannels of $\underline{d}$, which subsequently create estimation errors in the residual offset, $\tilde{\epsilon}_m$. Figure 6 shows the performance of the RFOCA in terms of Bit Error Rate (BER) vs SNR again in AWGN. The BER is virtually zero at values of SNR above 16 dB but suddenly increases below 16 dB. This result is a direct consequence of the threshold effect observed with the previous error variance results. It is observed that at an SNR of 16 dB only a few out of the total of 500 received bursts give rise to errors. However, these errors are significant giving rise to a high overall BER. Such occurances became more common when the SNR is reduced below 15 dB, thus increasing the BER very rapidly.

Appropriate models for BFWA channels are in the process of being defined. The Stanford University Interim (SUI) channels comprise 6 models for 3 different terrain conditions [13]. All of them are simulated using 3 taps, each having either Rayleigh or Ricean amplitude distributions. The channel is assumed to be wide-sense stationary uncorrelated scattering (WSSUS) and each tap of the CIR is modeled as $h_i = \beta_i e^{j\phi_i}$, where the amplitude β_i and the phase ϕ_i are selected independently [14]. The burst takes less than 10 ms to transmit at the selected sampling frequency, consequently the channel is assumed constant for the duration of each burst. We have selected the SUI-2 channel model, pertaining to terrains with low tree densities and with antennas having a directivity of 30 degrees at the SU and 120 degrees at the BS. The channel is characterised by a RMS delay spread of 0.2 μs.

Figure 7 allows a comparison of the error variances of the SCA

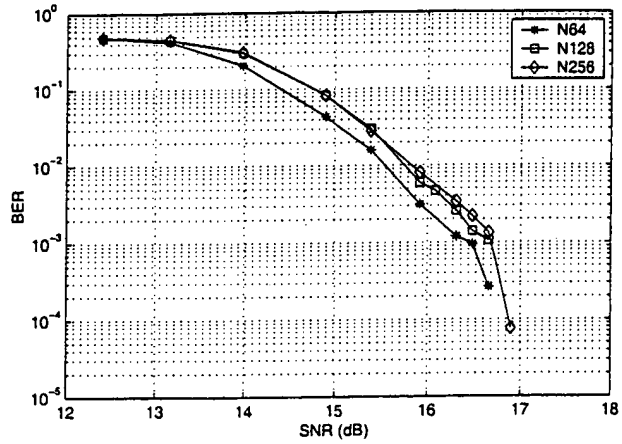

Fig. 6. Performance of RFOCA in AWGN for $N = 64, 128, 256$ and $\epsilon = 0.5$

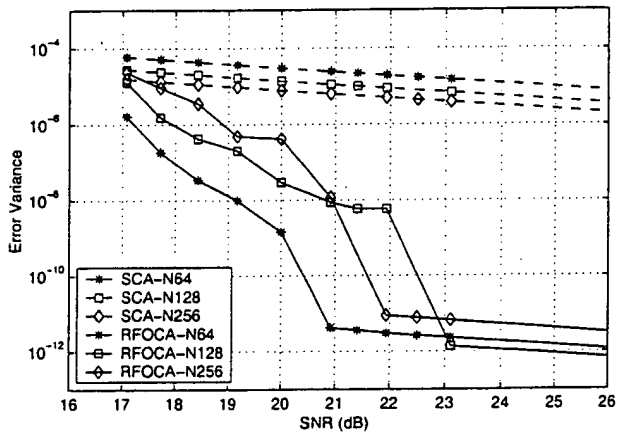

Fig. 7. Comparison of Error Variances of SCA and RFOCA with AWGN and SUI-2 CIR for $N = 64, 128, 256$ and $\epsilon = 0.5$

and the RFOCA for an OFDM system with $\epsilon = 0.5$ in the SUI-2 channel. A new channel in accordance with the SUI-2 profile is randomly generated for the transmission of each burst. The RFOCA error variance is seen to be many orders of magnitude lower than at the end of the acquisition stage despite the presence of the SUI-2 channel.

Figure 8 shows the performance of the RFOCA in terms of BER vs SNR for the SUI-2 channel and $\epsilon = 0.5$. The threshold effect now occurs at an SNR in the region of 20 dB owing to the effect of the SUI-2 channel.

VI. Conclusion

We have presented a Residual frequency Offset Correction Algorithm (RFOCA), that compliments the frequency acquisition process performed by the Schmidl and Cox Algorithm (SCA). The RFOCA continuously tracks and compensates for the residual frequency offset that is present after the acquisition stage. We have applied the RFOCA for AWGN and BFWA channels, namely the SUI-2 channel profile, and have shown a significant reduction in the error variance brought about by the use of the RFOCA following the initial acquisition stage. Although the algorithm may appear to suffer from a threshold effect it still gives a significant

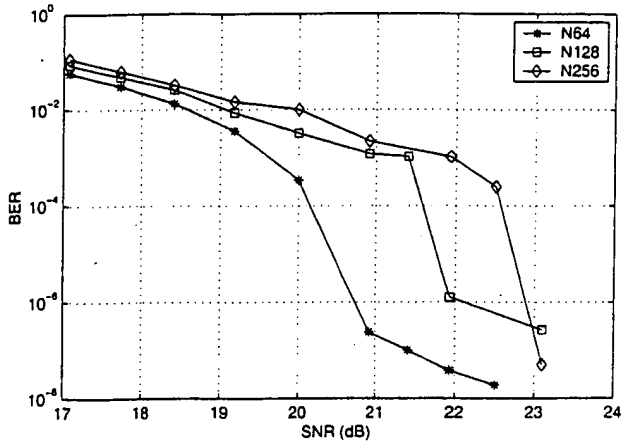

Fig. 8. Performance of RFOCA with AWGN and SUI-2 CIR for $N = 64, 128, 256$ and $\epsilon = 0.5$

performance advantage at realistic signal to noise ratios. In the future we hope to address the threshold effect by improving the phase unwrapping and investigating other criteria for the selection of the subchannels. We also hope to improve the performance of the SCA in a frame synchronisation role.

References

[1] ETSI, *Broadband Radio Access Networks (BRAN); HIPERLAN-2; Physical Layer*, April 2000.

[2] R. van Nee, G. Awater, M. M. H. Takanashi, M. Wester, and K. Halford, "New high-rate wireless LAN standards," *IEEE Communication Magazine*, vol. 37, pp. 82–88, December 1999.

[3] A. Peled and A. Ruiz, "Frequency domain data transmission using reduced computationally complexity algorithms," in *Proceedings of IEEE International Conference of Acoustics, Speech and Signal Processing*, (Denver), pp. 964–967, April 1980.

[4] V. S. Abhayawardhana and I. J. Wassell, "Frequency scaled time domain equalization for OFDM in broadband fixed wireless access channels," in *Proceedings of the IEEE Wireless Communications and Networking Confernce*, 2002. to be presented.

[5] T. M. Schmidl and D. Cox, "Robust frequency and timing synchronisation for OFDM," *IEEE Transactions on Communications*, vol. 45, pp. 1613–1621, December 1997.

[6] P. H. Moose, "A technique for orthogonal frequency division multiplexing frequency offset correction," *IEEE Transactions in Communications*, vol. 42, pp. 2908–2914, October 1994.

[7] Y. Zhao and S.-G. Haggman, "Intercarrier interfernce self-cancellation scheme for OFDM mobile communication systems," *IEEE Transactions on Communications*, vol. 49, pp. 1185–1191, July 2001.

[8] H. Nogami and T. Nagashima, "A frequency and timing period acquisition technique for OFDM systems," in *Proceedings of Personal, Indoor and Mobile radio Communication (PIMRC)*, pp. 1010–1015, Spetember 1995.

[9] J.-J. van de Beek and M. Sandell, "ML estimation of time and frequency offset in OFDM systems," *IEEE Transactions on Signal Processing*, vol. 45, pp. 1800–1805, July 1997.

[10] J. Armstrong, "Analysis of new and existing methods of reducing intercarrier interference due to carrier frequency offset in OFDM," *IEEE Transactions on Communications*, vol. 47, pp. 365–369, March 1999.

[11] H. Kobayashi, "A novel coherent demodulation for M-QAM OFDM signal operating in the burst mode," in *Proceedings of the IEEE Vehicular Technology Conference (Fall)*, vol. 3, pp. 1387–1391, September 2000.

[12] H. Meyr, M. Moeneclaey, and S. Fechtel, *Digital Communication Receivers; Synchronization Channel Estimation and Signal Processing*. John Wiley & Sons Inc., 1998.

[13] V. Erceg, K. Hari, *et al.*, "Channel models for fixed wireless applications," tech. rep., IEEE 802.16 Broadband Wireless Access Working Group, January 2001.

[14] K. Pahlavan and A. Levesque, *Wireless Information Networks*. New York: J. Wiley & Sons, 1995.

A Novel Intercarrier Interference Cancellation Approach in OFDM based on BSS

Yuan Liu and Wasfy Mikhael
Department of Electrical and Computer Engineering
University of Central Florida
Orlando, FL, 32816, USA

Abstract- Orthogonal Frequency Division Multiplexing (OFDM) is widely applied in wireless communication systems nowadays. In practice, there are frequency differences between the local oscillators in the transmitter and in the receiver. Due to these frequency offsets, the sub-carriers are not orthogonal. This leads to InterCarrier Interference (ICI) between the sub-carriers and degrades the system performance severely.

In this contribution, we propose a new ICI cancellation method based on Blind Source Separation (BSS). The relative gradient algorithm is employed to produce the separating matrix. Also, a technique to solve the permutation ambiguity is developed. The algorithm's interference cancellation is maintained for a wide range of interference conditions. Computer simulations are given, which confirm the effectiveness of the proposed compensation technique.

1. Introduction

In OFDM communication systems, a wideband source signal is partitioned into a number of the narrow sub-signals which are transmitted simultaneously employing the orthogonal sub-carriers. OFDM has various applications in wireless communications, such as digital audio, digital TV [1], and broadband satellite communication [2]. One major limitation of OFDM in many applications is its sensitivity to frequency differences between the local oscillators in the transmitter and in the receiver. These frequency offsets cause crosstalk between the sub-carriers, namely, ICI. ICI increases the Symbol Error Rate (SER) of the demodulated signal and degrades the performance of the receiver [3,4].

Zhao and Haggman have proposed ICI self-cancellation scheme to mitigate the ICI effects [5]. The resulting system is less bandwidth efficient than the normal OFDM scheme [5,6].

In this paper, an InterCarrier Interference Cancellation approach based on BSS (ICI/BSS) is proposed. In addition, a technique is given to solve the permutation ambiguity inherent in BSS type algorithms, which makes ICI/BSS practical in practice. Another advantage of ICI/BSS is that no prior information is needed. Also, no training sequences are required, which leads to efficient utilization of the bandwidth.

This paper is organized as follows. For a perfect Nyquist channel, the model of ICI resulting from the frequency offsets is described in detail in Section 2. ICI/BSS employing the relative gradient algorithm is given in Section 3. The technique to solve the permutation ambiguity is also given in Section 3. In Section 4, simulation results are given. Conclusions are drawn in Section 5.

2. Mathematical Formulation

The complete block diagram of the transceiver for OFDM system is given [1]. In this paper, the analysis considers only the impairments due to the frequency offsets. Thus, the forward error correct coding bock is not included. The frequency offsets alone do not cause InterSymbol Interference (ISI).

Usually, a cyclic prefix is used to eliminate the ISI in OFDM. The use of a cyclic prefix is not considered in this analysis too.

The structure of the simplified OFDM system, used to derive the ICI mathematical model, is shown in Fig. 1. In OFDM, interleaving is applied to correct bit errors, which occurs in burst rather being randomly scattered. A common used interleaving scheme is block interleaving, where input bits are written into a block column by column and read out row by row. The length of the block's column equals several times of the symbol length [7]. After interleaving, the serial source signal s(n) is independent at the time instant n. In general, s(n) is assumed to be complex-valued, zero-mean, stationary, and nongaussian distributed. The symbol time of s(n) is T_s. In Fig.1, the parallel source signals $s_i(m)$ (i=0,1,...,N-1) are given by

$$s_i(m) = s(iN + m) \tag{1}$$

where N is the number of the sub-carriers.

The symbol time of $s_i(m)$ is T_p, which is related to T_s as

$$T_p = NT_s \tag{2}$$

Since s(n) is white in the time domain, the signals $s_i(m)$ are considered to be mutually independent.

Then, N points Inverse Discrete Fourier Transform (IDFT) is applied to modulate $s_i(m)$ into the orthogonal sub-carriers. The modulated orthogonal signals $b_k(m)$ (k=0,1,...,N-1) are given by

$$b_k(m) = \frac{1}{N}\sum_{i=0}^{N-1} s_i(m)\exp\left(\frac{j2\pi ki}{N}\right) \tag{3}$$

where k is the IDFT index.

The signal b(n) is obtained from $b_k(m)$ by parallel to serial operation. The transmitted signal $s_T(t)$ is given by

$$s_T(t) = \exp(j2\pi f_c t)\sum_{n=-\infty}^{+\infty} b(n)g_T(t - nT_s) \tag{4}$$

where f_c is the local oscillator frequency, and $g_T(t)$ is the impulse response of the low-pass filter, in the transmitter.

To simplify the following analysis, the additive white gaussain noise n(t) is ignored in the derivation. The received signal $s_R(t)$ is given as

$$s_R(t) = s_T(t) \otimes h(t) \tag{5}$$

where h(t) is the impulse response of the channel and $\otimes$ denotes convolution.

In the receiver side, the local oscillator frequency is $f_c + \Delta f$, which is different from the transmitter side by Δf. The phase delay between the local oscillators in the transmitter and in the receiver is ignored. Thus, after the demodulation by $f_c + \Delta f$ and the low-pass filter $g_R(t)$, in the receiver, the signal $c(t)$ is given by

$$\begin{aligned} c(t) &= \exp(-j2\pi\Delta f t)\sum_{n=-\infty}^{+\infty} b(n)g_T(t - nT) \otimes h(t) \otimes g_R(t) \\ &= \exp(-j2\pi\Delta f t)\sum_{n=-\infty}^{+\infty} b(n)p(t - nT) \end{aligned} \tag{6}$$

where $g_R(t)$ is the impulse response of the low-pass filter in the receiver and p(t) is the combined impulse response of the transmitter filter, the channel filter, and the receiver filter.

Assuming that p(t) satisfies the Nyquist pulse-shaping criterion for samples taken at the optimum instants of intervals T_s [6]. After ADC and serial to parallel block in the receiver, the signals are

given by

$$c_k(m) = \exp\left(j2\pi\Delta f k T_s\right) b_k(m) = \exp\left(\frac{j2\pi ke}{N}\right) b_k(m) \tag{7}$$

where the frequency error is defined

$$e = N\Delta f T_s = \Delta f T_p \tag{8}$$

N points Discrete Fourier Transform (DFT) is applied to the signals, $c_k(m)$, to produce the demodulated signals

$$\begin{aligned} x_i(m) &= \sum_{k=0}^{N-1} c_k(m) \exp\left(\frac{-j2\pi kl}{N}\right) \\ &= \frac{1}{N} \sum_{i=0}^{N-1} s_i(m) \sum_{k=0}^{N-1} \exp\left(\frac{-j2\pi k(i-l+e)}{N}\right) \\ &= \frac{1}{N} \sum_{i=0}^{N-1} \alpha_{l,i} s_i(m) \end{aligned} \tag{9}$$

where the coefficient $\alpha_{l,i}$ is given by

$$\alpha_{l,i} = \frac{\sin\left[\pi\left(i-l+e\right)\right]}{N\sin\left[\frac{\pi(i-l+e)}{N}\right]} \exp\left[j\pi\left(\frac{N-1}{N}\right)\left(i-l+e\right)\right] \tag{10}$$

The relationship between the demodulated signals $x_i(m)$ and the parallel source signals $s_i(m)$ can be expressed in matrix format as follows

$$X(m) = AS(m) \tag{11}$$

where

$$X(m) = \left[x_0(m), \ldots, x_i(m), \ldots, x_{N-1}(m)\right]^T \tag{12}$$

$$S(m) = \left[s_0(m), \ldots, s_i(m), \ldots, s_{N-1}(m)\right]^T \tag{13}$$

and the mixing matrix is given by

$$A = \begin{pmatrix} \alpha_{0,0} & \cdots & \alpha_{0,N-1} \\ \vdots & \ddots & \vdots \\ \alpha_{N-1,0} & \cdots & \alpha_{N-1,N-1} \end{pmatrix} \tag{14}$$

If there are no frequency offsets, $\Delta f = 0$, $\alpha_{l,i} = 1\ (l = i)$ and $\alpha_{l,i} = 0\ (l \neq i)$. Thus, the matrix A is the identity matrix. Thus, no ICI occurs. If $\Delta f \neq 0$, $\alpha_{l,i}\ (i \neq l)$ will not equals zero, which results in ICI. The value of $\alpha_{l,i}$ depends on the frequency error e and on $(i-l)$ mod N, where mod is modulus after division, instead of directly on l and i. Hence, the mixing matrix A is a circulant matrix, and the inverse matrix of A is also a circulant matrix [8]. Also, all the diagonal elements of A are equivalent. Usually, in practice the frequency offsets are very small. Hence, $e \ll 1$ and

$$\left|\alpha_{i,i}\right| \gg \left|\alpha_{i,l}\right|, i \neq l \tag{15}$$

In other words, the absolute values of the diagonal elements in the matrix A are greater than the

off-diagonal ones. For the wide ranges of the frequency error, $-0.4 \le e \le 0.4$, and of the sub-carrier number, $4 \le N \le 52$, the absolute value of the diagonal element and the maximum absolute value of the off-diagonal elements are shown in Fig. 2. It is obvious that equ. (15) is generally valid in practice. This property is also held for the inverse matrix A, which is shown on Fig. 3.

3. Proposed ICI/BSS Approach

Usually, whitening is first applied before the BSS algorithm. X(m) is whitened by a whitening matrix Q to produce a white measurement signal vector $\tilde{X}(m)$,

$$\tilde{X}(m) = QX(m) = D^{-1/2}EX(m) \tag{16}$$

where D is the diagonal matrix of eigenvalues and E is the matrix of the eigenvectors of the covariance matrix R_{xx} of $X(m)$.

After whitening, the mixing model is given by

$$\tilde{X}(m) = QAS(m) = \tilde{A}S(m) \tag{17}$$

where the new mixing matrix $\tilde{A}$ is orthonormal.

To estimate an orthonormal mixing matrix greatly reduces the complexity of the BSS algorithm afterwards [8]. Then, the relative gradient method is used to determine the separating matrix $\tilde{W}$, which transforms the white measurement signals $\tilde{x}_i(m)$ into the estimates of the source signals $\tilde{s}_i(m)$. The update rule for the separating matrix $\tilde{W}$ is given by [10]

$$\tilde{W} = \tilde{W} + \mu\left[I - E\left(f\left(\tilde{S}(r)\right)\cdot\tilde{S}(r)^H\right)\right]\times\tilde{W} \tag{18}$$

where μ is the convergence factor, I is the identity matrix, $E(\ )$ denotes expectation, and the superscript H denotes conjugate transpose. The estimate source signal vector

$$\tilde{S}(m) = \tilde{W}\tilde{X}(m) = \left[\tilde{s}_1(m),\ldots,\tilde{s}_i(m),\ldots,\tilde{s}_{N-1}(m)\right]^T \tag{19}$$

and the nonlinear function

$$f\left(\tilde{S}(m)\right) = [f(\tilde{s}_1(m)),\ldots,f(\tilde{s}_i(m)),\ldots,f(\tilde{s}_{N-1}(m))]^T \tag{20}$$

The advantage of the relative gradient method is its equivarient property, namely, the performance of the relative gradient method does not depend on the mixing matrix [11].

After each iteration of the relative gradient method, the separating matrix $\tilde{W}$ is made to be orthonormal by the symmetric orthonormalization method [9].

$$\tilde{W} = \tilde{W}\left(\tilde{W}^H\tilde{W}\right)^{-\frac{1}{2}} \tag{21}$$

The separating matrix corresponding to the original matrix A is given by

$$W = \tilde{W}Q \tag{22}$$

The BSS type algorithm is associated with the permutation and gain ambiguities, which need to be resolved in the application. In other words, the separating matrix W is related to the mixing matrix A by

$$WA = \Lambda P \tag{23}$$

where P is the permutation matrix and Λ is the diagnose matrix given by

$$\Lambda = \begin{pmatrix} \beta_0 & \cdots & 0 \\ \vdots & \ddots & \vdots \\ 0 & \cdots & \beta_{N-1} \end{pmatrix} \tag{24}$$

where g_i is the unknown complex number.

The technique to solve the permutation ambiguity is given as follows. If W is without the permutation ambiguity, the separating matrix W is also in same format as the mixing matrix A, namely,

$$|w_{i,i}| \square |w_{i,l}|, i \neq l \tag{25}$$

The row permutation is applied to the separating matrix W to change its format to satisfy equ. (25). In this way, the permutation is solved successfully, and the compensated source signals are given by

$$\hat{S}(m) = WX(m) \tag{26}$$

where the parallel compensated signal vector

$$\hat{S}(m) = [\hat{s}_0(m), ..., \hat{s}_i(m), ..., \hat{s}_{N-1}(m)]^T \tag{27}$$

To resolve the gain ambiguity, additional information is needed to be embedded into the data streams. This information is usually in the form of predefined symbol sequences, which is used at the receiver detector to solve the gain ambiguity [9,12]. The whole ICI/BSS compensation scheme is summarized in Table 1.

4. Simulation Results

The performance of the proposed algorithm is evaluated through the computer simulations. In the simulated OFDM system, the number of sub-carriers N equals 8. For each of the parallel source signals $s_i(m)$, 30,000 samples of the baseband QPSK modulated signals are used, which are the statistically independent. In the relative gradient algorithm, the convergence factor μ equals 0.04. Also, the nonlinear function $f(y) = |y|^2 y$ is a good choice, since the typical baseband digital communication signals are complex with a negative kurtosis [13]. The effectiveness of ICI/BSS is demonstrated by comparing SER of the compensated signal $\hat{s}(n)$ with SER of the uncompensated signal $\hat{s}'(n)$, which is obtained from $x_i(m)$ by parallel to serial operation.

For 10dB signal-to-noise ratio (SNR), SER of $\hat{s}(n)$ and $\hat{s}'(n)$ vs the frequency error is given as Fig. 4. It is obvious the performance degradation due to the frequency offsets from the SER curve of $\hat{s}'(n)$. At the point $e = 0$, SER of $\hat{s}(n)$ and $\hat{s}'(n)$ are equivalent, which means ICI/BSS does not degrade the system performance if there are not the frequency offsets. From $e = 0$ to $e = 0.2$, SER of $\hat{s}(n)$ is almost constant, which means the effect of ICI is successfully removed after the compensation of ICI/BSS.

Under the fixed frequency offset $e = 0.1$, SER of $\hat{s}(n)$ and $\hat{s}'(n)$ vs SNR is given as Fig. 5. Thus, under the different noise levels, ICI/BSS is still effective and can greatly improve the system performance.

5. Conclusions

In this paper, the ICI model due to the frequency offsets for the perfect Nyquist channel in OFDM is derived. A compensation scheme for ICI in OFDM employing the BSS algorithm, namely, ICI/BSS is proposed. A practical technique is presented to solve the permutation ambiguity. This approach utilizes the bandwidth efficiently and does not require any prior information about the system. The simulation results confirmed the excellent properties of ICI/BSS in compensating the frequency offsets over a wide range. Also, the performance was maintained under different noise levels.

Reference

[1]. Richard van Nee, and Ramjee Prasad, OFDM for Wireless Multimedia Communications, Artech House Publisher, 2000

[2]. Muli Kifle, Monty Andro, Mark J. Vanderaar, "An OFDM System Using Polyphase Filter and DFT Architecture for Very High Data Rate Application," NASA document, http://gltrs.grc.nasa.gov/GLTRS

[3]. Thierry Pollet, Mark Van Bladel, and Marc Moeneclaey, "BER Sensitivity of OFDM System to Carrier Frequency Offset and Wiener Phase Noise," IEEE Trans. on Communication, Vol. 43, No. 2/3/4, pp. 191-193, Feb./March/April, 1995

[4]. Fu Qing, and Monty Andro, "The Effect of Doppler Frequency Shift, Frequency Offset of the Local Oscillator, and Phase Noise on The Performance of Coherent OFDM Receivers," NASA document, http://gltrs.grc.nasa.gov/GLTRS

[5]. Yuping Zhao, and Sven-Gustav Haggman, "Intercarrier Interference Self-Cancellation Scheme for OFDM Mobile Communication System," IEEE Trans. on Communication, Vol. 49, No. 7, pp.1185-1191, July 2001

[6]. Jean Armstrong, "Analysis of New and Existing Methods of Reducing Intercarrier Interference Due to Carrier Frequency Offset in OFDM," IEEE Trans. on Communication, Vol. 47, No. 3, pp. 365-369, March, 1999

[7]. Bernard Sklar, Digital Communications: Fundamental and Application, Second Edition, Prentice Hall, 2001

[8]. Robert M. Gray, Toeplitz and Circulant Matrices: A Review, http://www-ee.stanford.edu/~gray/toeplitz.pdf, August 2003

[9]. Hyvärien, J. Karhunen and E. Oja, Independent Component Analysis, John Wiley & Sons, Inc., 2001.

[10].S-I. Amari, T-P. Chen, and A.Cichocki, "Stability Analysis of Learning Algorithms for Blind Source Separation", Neural Networks, vol.10, no.8, pp. 1345–1351, August, 1997

[11].Jean-Francois Cardoso, and Beate Hvam Laheld, "Equivariant Adaptive Source Separation," IEEE Trans. on Signal Processing, Vol. 44, No.12, pp. 3017-303, Dec. 1996

[12].Ivica Kostanic and Wasfy Mikhael, "Independent Component Analysis Based QAM Receiver", accepted for publication in Digital Signal Processing – A Review Journal

[13].Shun-ichi Amari, S. C. Douglas, A. Cichocki, and H. H. Yang, "Multichannel Blind Deconvolution and Equalization Using the Natural Gradient", Signal Processing Advance in Wireless Communication Workshop, pp. 101-104, Paris, 1997

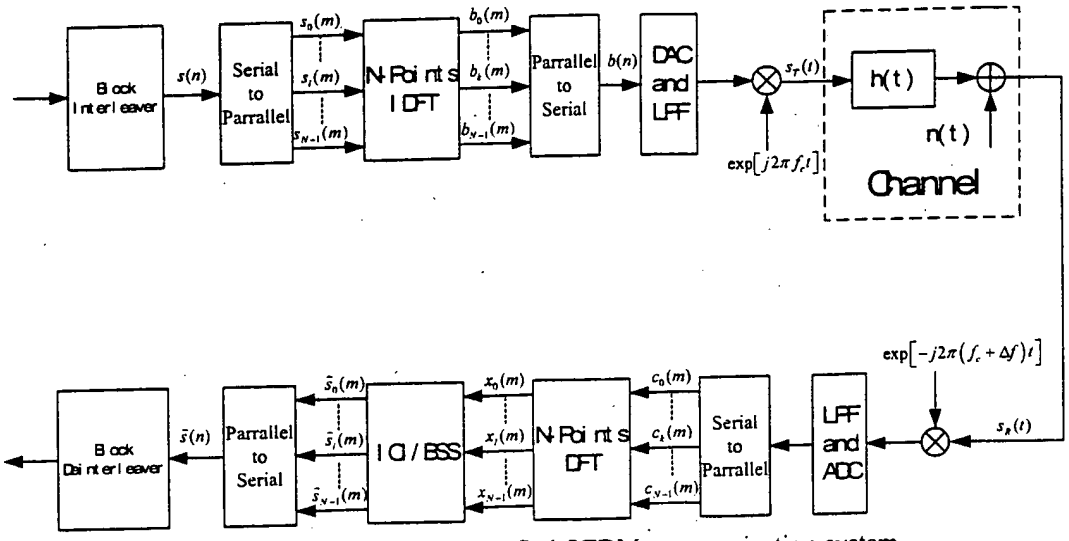

Fig.1: Structure of a simplified OFDM communication system

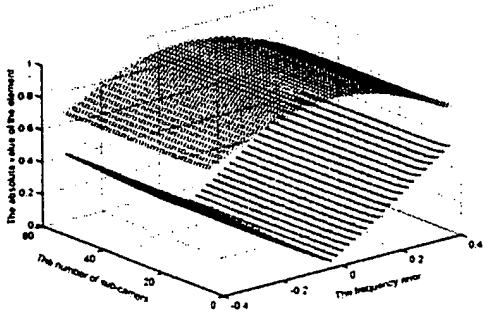

O The absolute value of the diagonal element

* The maximum absolute value of the off-diagonal elements

Fig.2: The absolute value of the diagonal and the maximum absolute value of the off-diagonal elements of the mixing matrix A, for the frequency error $-0.4 \le e \le 0.4$, and the sub-carrier number $4 \le N \le 52$

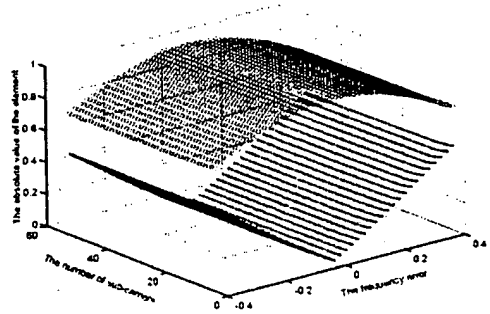

O The absolute value of the diagonal element

* The maximum absolute value of the off-diagonal elements

Fig.3: The absolute value of the diagonal and the maximum absolute value of the off-diagonal elements of the inverse matrix of the mixing matrix A, for the frequency error $-0.4 \le e \le 0.4$, and the sub-carrier number $4 \le N \le 52$

Step 1. Whiten of X(m) through a linear transform, equ. (16).

Step 2. Initialize the matrix $\tilde{W}$ as a random matrix.

Step 3. Update $\tilde{W}$ by the relative gradient algorithm to, equ.(18).

Step 4. Orthonormalize $\tilde{W}$, equ.(21).

Step 5. Check the convergence of $\tilde{W}$, and if the convergence is not reached go back to Step 3, otherwise finish the iterations.

Step 6. Obtain the separating matrix W, equ.(22).

Step 7. Solve the permutation ambiguity of the separation matrix W.

Step 8. Obtain the compensated signal vector, equ.(26).

Table 1. Outline of the proposed ICI/BSS approach

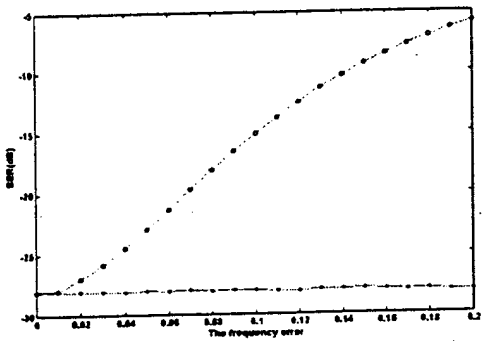

O SER of $\hat{s}'(n)$

* SER of $\hat{s}(n)$

Fig.4: SERs vs. the frequency error

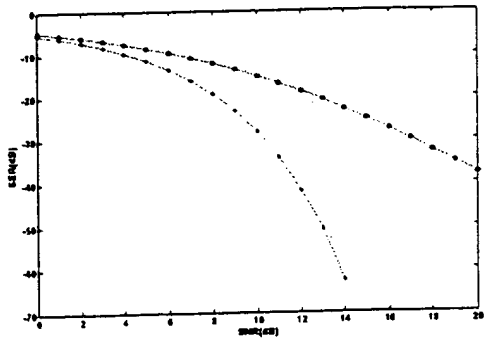

O SER of $\hat{s}'(n)$

* SER of $\hat{s}(n)$

Fig.5: SERs vs. SNR